JOURNAL OF MATERIALS PROCESSING TECHNOLOGY 201 (2008) 791–793

available at www.sciencedirect.com

ScienceDirect

journal homepage: www.elsevier.com/locate/jmatprotec

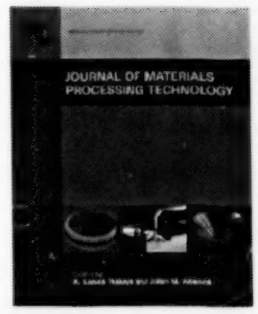

Author Index of Volume 201

Abou-El-Hossein, K.A., 483
Abudollah, A., 43
Aghili, A., 133
Amin, A.K.M.N., 466
Amini, S., 43
Amirsadeghi, A., 673
An, C.-C., 706
Awais, M., 73
Azushima, A., 390

Bae, J.W., 336
Bae, W.B., 742
Barišić, B., 786
Barreiros, F.M., 651
Batalha, G.F., 507
Bergheau, J.M., 450, 590
Bielańska, E., 291
Bonnet, C., 450
Brahmankar, P.K., 380
Brosse, A., 590
Burhanuddin, Y., 570
Byon, S.M., 73, 106

Castanho, J.M., 651
Cha, K.-U., 491
Chan, L.C., 413
Chang, C.-J., 14
Chang, C.K., 565
Chang, H.Y., 560
Chang, J.H., 560
Chang, J.K., 689
Chang, J.R., 252
Chang, Q., 736
Chang, R.C., 770
Chao, C.K., 770
Che Haron, C.H., 570
Chen, C.-C.A., 606
Chen, C.-H., 618
Chen, F.-K., 150, 247
Chen, G.Z., 689
Chen, H.-Y., 297
Chen, J.-Y., 618
Chen, R.-H., 706
Chen, Y.-S., 37
Cheng, C.H., 554, 683
Cheng, Y.-L., 640
Chiu, N.-H., 601
Cho, C., 678
Cho, C.D., 179
Cho, G.-J., 761
Cho, J.R., 168, 742
Cho, S.-Y., 60
Choi, B.H., 526
Choi, B.K., 526
Choi, J.-H., 261
Choi, J.H., 742
Choi, K.-K., 580
Choi, S., 91, 112, 348
Choi, Y.-M., 497
Chong, M.K., 746
Chou, C.C., 542
Chu, K.Y., 770
Chuang, C.T., 770
Chuang, W.-C., 150

Díez, E., 486
Dobrzański, L.A., 291, 310
Dolah, S.B., 466
Donati, L., 156
Drygała, A., 291

Ekreem, N.B., 780
Endo, R., 401
Engel, U., 2
Eom, I.S., 515

Fang, G., 226
Fujiwara, W., 720
Fukauara, K., 319
Fukuzawa, Y., 401
Furushima, T., 123
Furuya, T., 536

Gao, L., 413
Gao, W.M., 629
Ghani, J.A., 570
Ghazali, M.J., 662
Gilles, P., 450
Gołombek, K., 291, 310
Goodarzi, M., 189
Gu, G., 97
Guao, Y.-Y., 601
Gujar, T.P., 775
Gweon, D.-G., 497

Ha, S.K., 425
Ha, Y.S., 168
Habeeb, H.H., 483
Haghi, A.K., 669
Hamdi, H., 450, 590
Han, J.Y., 742
Harada, Y., 319
Hashmi, M.S., 369
Hashmi, M.S.J., 645
Hertel, K., 242
Higashi, K., 395
Hino, R., 395
Hirota, K., 209
Ho, H.-L., 14
Hocheng, H., 471, 560
Hodgson, P.D., 303, 629
Hong, J.K., 419, 515
Hong, S.-K., 491
Hoque, A.S.M., 204
Horita, Z., 32
Hort, N., 359
Hsiang, S.H., 138
Hsiang, S.-H., 14
Hsu, L.-S., 606
Hsu, R.Q., 252
Hsu, T.H., 683
Hsu, Y.-C., 128
Hu, H., 364
Hu, L., 736
Huang, J.-C., 477
Huang, L., 267
Huang, S.-J., 297
Huang, Y.-M., 256, 385
Huang, Y.X., 689
Hung, C., 751
Hung, J.-C., 751
Huynh, N.N., 79
Hwang, M.Y., 112
Hwang, Y.M., 174

Im, Y.T., 1, 19, 73, 91, 348
Imai, K., 193
Itadani, M., 720

Jan, F.-S., 145
Jane Wang, Q., 85
Jang, Y.C., 419
Jeong, H.G., 179
Jeong, S.H., 118
Jeong, S.-T., 761
Ji, Y.H., 354
Jiang, Z.Y., 85
Jin, Y., 189, 193
Jo, H., 53
Jo, H.H., 53
Jogi, B.F., 380
Joko, K., 390
Joo, J.-W., 261

Elsevier B.V.
doi:10.1016/S0924-0136(08)00270-7

Joo, O.-S., 775
Jung, H.Y., 742
Jung, K.-D., 775

Kadirgama, K., 483
Kainer, K.U., 359
Kang, B.S., 746
Kang, C.G., 336
Kang, C.Y., 515
Kang, I.S., 585
Kang, K.W., 425
Kang, M.C., 331, 585
Kang, M.J., 502
Kang, S.H., 431, 436
Katayama, I., 401
Kavamura, H.A., 507
Keh, C.-C., 128
Kelleher, M.C., 645
Kermansaravi, F., 725
Khan, A.A., 325
Kim, B.G., 716
Kim, B.M., 53, 273
Kim, C., 521
Kim, C.W., 425
Kim, D.W., 419
Kim, E.-Z., 163
Kim, E.Z., 179
Kim, G.H., 118
Kim, H.J., 101
Kim, H.S., 19, 32, 425
Kim, I.S., 635
Kim, J., 521, 746
Kim, J.H., 168
Kim, J.-H., 491
Kim, J.S., 331, 585
Kim, J.W., 755
Kim, J.-Y., 261
Kim, K., 497
Kim, M.B., 515
Kim, N., 710
Kim, S.I., 106
Kim, S.j., 761
Kim, S.K., 445
Kim, S.M., 746
Kim, S.W., 431
Kim, S.-Y., 25
Kim, T.H., 118, 168
Kim, Y.S., 596
Kiuchi, M., 623
Ko, D.C., 273
Ko, S.L., 454
Kobayashi, N., 531
Kohamada, S., 319
Kohzu, M., 395
Kong, L.X., 629
Koyama, J., 193
Ku, T.W., 746
Kuboki, T., 189
Kubota, S., 25
Kuo, K.-L., 48
Kuwabara, T., 232
Kwak, J.S., 596
Kwan, C.-T., 145
Kwang-Sup, S., 574
Kwon, H.C., 73
Kwon, Y.N., 431

Lai, J.-H., 640
Lajis, M.A., 466
Lang, L., 97
Lee, B.-Y., 618
Lee, D.G., 716, 755
Lee, D.L., 19, 91, 348
Lee, G.A., 112
Lee, H.C., 19, 348
Lee, H.-S., 280, 678
Lee, H.S., 68
Lee, H.W., 73, 112
Lee, I.S., 273
Lee, J., 710
Lee, J.-B., 60
Lee, J.D., 91
Lee, J.H., 431, 436
Lee, J.M., 53
Lee, K.H., 331
Lee, K.S., 445
Lee, K.U., 454
Lee, K.Y., 585
Lee, M.G., 497
Lee, S., 441
Lee, S.-C., 761
Lee, S.H., 53, 118, 542
Lee, S.M., 336
Lee, S.Y., 348
Lee, W.-C., 145
Lee, Y., 106, 348, 419
Lee, Y.-S., 163
Lee, Y.S., 431, 436
Lee, Y.-S., 491, 580
Lei, L.P., 226
Li, C.-L., 237, 256, 385
Li, D., 736
Li, L., 746
Li, N., 364
Li, T., 97
Li, Y., 408
Liang, D.L., 252
Liao, C.-C., 247
Liao, Y.S., 460
Lim, H., 521
Lim, S.J., 179
Lin, C.J., 689
Lin, C.-S., 612, 657
Lin, H.M., 460
Lin, H.-S., 128
Lin, K.-H., 701
Lin, S.-T., 612, 657, 701
Lin, W.-S., 374
Lin, Y.-C., 701
Lin, Y.W., 138
Lin, Z.-C., 477
Liu, C.-H., 37
Liu, Q., 303
Liu, X.H., 79
Liu, Y., 267
Lu, C., 79
Lu, Y.-H., 237

Mabuchi, T., 214
Maeda, R., 548
Mahfouf, M., 101
Mahmud, M.B., 466
Majzoobi, G.H., 133
Manabe, K., 123
Manabe, K.-i., 214
Martins, A.G., 651
Matos, M., 651
Mazlan, S.A., 780
Mikuła, J., 310
Mirzai, M.A., 214
Mohammad, B., 483
Mohammadi, K., 669
Mridha, S., 325
Murata, M., 189
Mustafa, A.H., 369

Na, K.H., 112
Na, K.-H., 163
Nagasawa, S., 401
Nahavandi, S., 629
Naisson, P., 590
Naka, T., 395
Nam, W.-J., 580
Nanda, V.S., 380
Nategh, M.J., 43
Nomura, M., 531, 536
Nozu, S., 720

Oh, S.-I., 163
Oh, Y.K., 64
Ohnishi, K., 720
Okuyama, C., 548
Olabi, A.G., 780
Omar, M.Z., 662
Osako, A., 315

Pakuła, D., 310
Palumbo, G., 183
Pan, W., 220
Pan, Y.-R., 695
Pancielejko, M., 310
Panek, P., 291
Papastathis, T.N., 198
Park, H.D., 73
Park, J.H., 331, 419, 425, 515
Park, J.-H., 491
Park, J.J., 354
Park, J.-N., 761
Park, J.W., 746
Park, N.K., 515
Pavlina, E.J., 242
Peng, Y., 736
Pérez, H., 486
Prasad, R.C., 380
Prasad, Y.V.R.K., 359
Praveen, P., 502
Puspitasari, I., 775

Qin, Y., 220

Rabizadeh, E., 725
Rainforth, W.M., 662
Rao, K.P., 359
Ratchev, S., 198
Rech, J., 450
Rios, J., 486
Ryll, M., 198

Sadeghi, M.H., 43
Sadighi, M., 725
Samin, R., 731
Saniee, F.F., 133
Saroosh, M.A., 19
Sato, T., 531

Sayuti, M., 731
Schikorra, M., 156
Seo, H.J., 118
Seol, D.Y., 336
Seong, Y.K., 570
She, F.H., 629
Shen, C.Y., 174
Sheu, J.J., 9
Shih, A., 560
Shimada, K., 536
Shin, H.J., 342
Shin, W.-J., 60
Shiou, F.J., 554
Si, L.Y., 79
Sladić, S., 786
Sohi, M.H., 673
Soković, M., 786
Soleimanimehr, H., 43
Son, I.H., 19, 91
Song, S.H., 746
Song, W.J., 746
Song, Y.S., 331
Sorgente, D., 183
Sugiyama, S., 623
Sulaiman, S., 731
Sun, C.Y., 226
Sun, Z., 364
Sunar, M., 369
Sung, B.S., 635
Sung, C.K., 765
Suresh Kumar Reddy, N., 574
Swee, C.Y., 570
Szecsi, T., 204

Takahashi, K., 189
Takahashi, M., 548
Tekkaya, A.E., 156
Tieu, A.K., 79, 85
Tomesani, L., 156
Torng, S., 150
Tricarico, L., 183
Tsai, H.-K., 247
Tsai, Y.-C., 751
Tsai, Y.-W., 256, 385
Tsai, Y.Y., 565
Tsao, C.C., 471
Tseng, C.-F., 374
Tseng, C.H., 565
Tsien, Y.C., 413
Tsuji, H., 720
Tsukiyama, Y., 209

Uchino, S., 401
Uemori, T., 395

Valiorgue, F., 450
Van Tyne, C.J., 242
Vieira, M.T., 651
Vizán, A., 486
Völkl, R., 2

Wagner, K., 2
Wang, A.-C., 37
Wang, C.-M., 37
Wang, J.H., 460
Wang, Z., 408
Won, T., 60
Wu, C.-H., 695
Wu, C.L., 765
Wu, Y., 531, 536

Xiong, S.W., 85
Xu, Y., 413

Yamamoto, K., 536
Yamamoto, M., 232
Yamanaka, M., 25
Yanagida, A., 390
Yanagimoto, J., 623
Yang, A.S., 683
Yang, C., 303
Yang, H., 267
Yang, H.D., 64
Yang, I.Y., 445
Yang, M., 315, 574
Yang, Y.-L., 612
Yang, Y.Y., 101
Yao, C.H., 765
Yarlagadda, P.K.D.V., 502
Yasuumi, T., 209
Ye, L., 303
Yeh, F.-H., 237
Yi, Y.-M., 280
Yi, Y.M., 68
Yilbas, B.S., 285, 369
Yoo, Y.T., 342
Yoon, D.J., 112, 179
Yoon, J.-H., 280
Yoon, J.H., 68
Yoon, S.C., 32
Yoshida, F., 395
Youn, S.-W., 548
Yu, C.H., 9

Zeng, P., 226
Zhan, M., 267
Zhang, S., 736
Zheng, P.F., 413
Zhou, M., 364
Zhou, X., 97
Zięba, P., 291
Żukowska, L.W., 310

JOURNAL OF MATERIALS PROCESSING TECHNOLOGY 201 (2008) 794–807

available at www.sciencedirect.com

ScienceDirect

journal homepage: www.elsevier.com/locate/jmatprotec

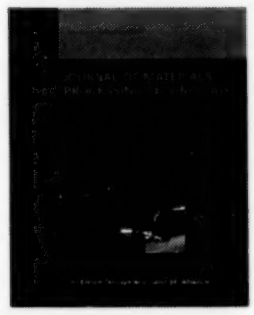

Subject Index of Volume 201

AA6060 alloy
Microstructure analysis of aluminum extrusion: Prediction of microstructure on AA6060 alloy, 156
ABAQUS
Effects of laminate sequencing on thermoforming of thermoplastic matrix composites, 725
Acidithiobacillus ferrooxidans
Metal removal rate of *Thiobacillus thiooxidans* without pre-secreted metabolite, 560
Acidithiobacillus thiooxidans
Metal removal rate of *Thiobacillus thiooxidans* without pre-secreted metabolite, 560
Acoustic emission
Tool condition and machined surface monitoring for micro-lens array fabrication in mechanical machining, 585
Acoustic emission (AE)
Effects of the laser treatment and thermal oxidation behavior of CoNiCrAlY/ZrO_2–8 wt%Y_2O_3 thermal barrier coating, 331
Adaptive
Prediction of work-hardening coefficient and exponential by adaptive inverse finite element method for tubular material, 413
Adaptive neural network controller
Ti6Al4V laser alloying process monitoring by using adaptive neural network controller, 297
Additive
Rheological behavior and tribological performance of a nanodiamond-dispersed lubricant, 542
AE signal
State classification of CBN grinding with support vector machine, 601
Aggregation
Rheological behavior and tribological performance of a nanodiamond-dispersed lubricant, 542
Air-blow
Prediction of slug carry-up by the punch in blanking by air-blow of the slug, 252
Al/SiC particulate metal–matrix composites
Experimental study of surface integrity during end milling of Al/SiC particulate metal–matrix composites, 574
Alloys 242
Effect of tool holder geometry and cutting condition when milling nickel-based alloy 242, 483
Al–Mg system alloy (AC7A)
A study on cooling characteristics of tire mold during a manufacturing process of Al–Mg system alloy casting mold, 64
Alumina
Effects of granule size and distribution on the cold isostatic pressed alumina, 657
A study on characterization of pack-cemented aluminide coating on metals, 669
Aluminium alloys
A comparative study of mechanically mixed layers (MMLs) characteristics of commercial aluminium alloys sliding against alumina and steel sliders, 662
Aluminum alloy
Formability of 6k21-T4 car panel sheet for viscoelastic–plastic flexible-die forming, 408
Aluminum alloy 6061
Some studies on fatigue crack growth rate of aluminum alloy 6061, 380
Aluminum nitride
Effects of reduction atmosphere and nano carbon powder addition on the deoxidization of injection molded aluminum nitride parts, 701
Approach and retract sequence
Planning and analysis of grinding processes for end mills of cemented tungsten carbide, 618
Arcan test
Mechanical strength evaluation for Nd-YAG laser and electric resistance spot weld (ERSW) joint under multiaxial loading, 507
Austempered ductile iron
Comparison of the influence of molybdenum and chromium TIG surface alloying on the microstructure, hardness and wear resistance of ADI, 673
Autofrettage
Machining effect of the autofrettaged compound cylinder under varying overstrain levels, 491
Axisymmetric drawing
Inhomogeneous deformation and residual stress in skin-pass axisymmetric drawing, 128
AZ31
Forming limit of AZ31 alloy sheet and strain rate on warm sheet metal forming, 431

Backward can extrusion
Backward can extrusion of ultra-fine-grained bulk Al–Mg alloy fabricated by cryomilling and hydrostatic extrusion, 163
Balanced flow
Finite element analysis of multi-hole extrusion of aluminum-alloy tubes, 150
Ball burnishing
Ultra-precision surface finish of NAK80 mould tool

Elsevier B.V.
doi:10.1016/S0924-0136(08)00271-9

steel using sequential ball burnishing and ball polishing processes, 554
Ball polishing
Ultra-precision surface finish of NAK80 mould tool steel using sequential ball burnishing and ball polishing processes, 554
Bar drawing
An investigation into the effect of redundant shear deformation in bar drawing, 133
Bending
Effect of hardening exponent on tube bending, 189
Creasing characteristic of aluminum foil coated paperboard, 401
Bending stiffness
Finite element modeling and simulation for bending analysis of multi-layer printed circuit boards using woven fiber composite, 746
Bidirectional extrusion
Forming characteristics of AZ31B magnesium alloy in bidirectional extrusion process, 179
Blanking
Precision blanking of thin sheet metals with the help of chemical etching, 209
Prediction of slug carry-up by the punch in blanking by air-blow of the slug, 252
Blowing agent
Development of microwave foaming method for phenolic insulation foams, 716
Bolt forming
Two-dimensional finite element approximation of the hexagonal bolt forming process, 19
Bolt forming process
Tool life prediction for the bolt forming process based on high-cycle fatigue and wear, 348
Buckling pressure
Buckling analysis and test of composite shells under hydrostatic pressure, 742
Bulge test
Hydraulic bulge testing of dual phase steel tubes produced using a novel processing route, 242
Burr
Development of deburring tool for burrs at intersecting holes, 454

Calibration
Numerical and experimental confirmation of the calibration stage's effect in multi-operation sheet hydroforming using poor-formability materials, 97
Car BIW
Mechanical strength evaluation for Nd-YAG laser and electric resistance spot weld (ERSW) joint under multiaxial loading, 507
Carbide tools
Behaviors of end milling Inconel 718 superalloy by cemented carbide tools, 460
Carbothermal reduction
Effects of reduction atmosphere and nano carbon powder addition on the deoxidization of injection molded aluminum nitride parts, 701
Carburization
The processing and fracture analysis on transmission shafts of a peanut harvester, 374
Case depth
The effects of process variables on the hardness of nitrided 3% chromium steel, 325
Casting defects
The molding analysis of automobile parts using the die-casting system, 635
CBN grinding
State classification of CBN grinding with support vector machine, 601
π-Cell
Numerical 3-D FEM simulation of tensor model for liquid crystal displays, 60
Chamfer
A study of improving warped characteristics during flange forging, 14
Charpy impact test
Effects of notch position of the Charpy impact specimen on the failure behavior in heat affected zone, 419
Chatter
Effects of workpiece preheating on surface roughness, chatter and tool performance during end milling of hardened steel D2, 466
Chemical bath deposition
Simple chemical method for nanoporous network of In_2S_3 platelets for buffer layer in CIS solar cells, 775
Chemolithotrophic
Metal removal rate of *Thiobacillus thiooxidans* without pre-secreted metabolite, 560
Chromium
Comparison of the influence of molybdenum and chromium TIG surface alloying on the microstructure, hardness and wear resistance of ADI, 673
CO_2 laser welding
Microstructures and mechanical properties of Inconel 718 welds by CO_2 laser welding, 515
Coated powders
Surface modification of stainless steel powders for microfabrication, 651
Coating
A study on characterization of pack-cemented aluminide coating on metals, 669
Cold cross-wedge rolling
Optimization of design parameters using a response surface method in a cold cross-wedge rolling, 112
Cold equal channel angular extrusion
Formability of steels subjected to cold ECAE process, 390
Cold forging
Tool life enhancement in cold forging by locally optimized surfaces, 2
Application of CAE in cold forging and heat treatment processes for manufacturing of precision helical gear part, 25
Cold isostatic pressing (CIP)
Effects of granule size and distribution on the cold isostatic pressed alumina, 657
Cold strip rolling
Modelling of the effect of friction on cold strip rolling, 85
Combined method
Development of a combined machining method using electrorheological fluids for EDM, 565
Compact tension (CT) specimens
Some studies on fatigue crack growth rate of aluminum alloy 6061, 380
Composite materials
A study on mechanical properties of carbon fiber reinforced plastics by three-point bending testing and transverse static response, 761
Composite shell
Buckling analysis and test of composite shells under hydrostatic pressure, 742

Compound cylinder
Machining effect of the autofrettaged compound cylinder under varying overstrain levels, 491
Compression
The study of injection/compression liquid composite molding, 695
Compression mode
An investigation of the behaviour of magnetorheological fluids in compression mode, 780
Compressive speed
An investigation of the behaviour of magnetorheological fluids in compression mode, 780
Computation time
Two-dimensional finite element approximation of the hexagonal bolt forming process, 19
Computational fluid dynamics
Integrated optimization system for high pressure die casting processes, 629
Condenser tube
Process analysis and die design in 12 cells condenser tube extrusion of Al3003, 53
Condition monitoring
Tool condition and machined surface monitoring for micro-lens array fabrication in mechanical machining, 585
Contact-free polishing
Fundamental performance of magnetic compound fluid polishing liquid in contact-free polishing of metal surface, 536
Controller
The energy absorption control characteristics of Al thin-walled tube under quasi-static axial compression, 445
Correlation analysis
Modelling of hot strip rolling process using a hybrid neural network approach, 101
Corrosion
A study on characterization of pack-cemented aluminide coating on metals, 669
CPU heat sink
Analysis of plastic flow and die design during extrusion of CPU heat sinks, 174
Crashworthiness
The energy absorption control characteristics of Al thin-walled tube under quasi-static axial compression, 445
Creasing rule
Creasing characteristic of aluminum foil coated paperboard, 401
Critical buckling load
Consideration of buckling characteristics for optimal design of stiffened punch in the blanking process of lead frame, 273
Cross plies
A study on mechanical properties of carbon fiber reinforced plastics by three-point bending testing and transverse static response, 761
Cryogenic milling
Backward can extrusion of ultra-fine-grained bulk Al–Mg alloy fabricated by cryomilling and hydrostatic extrusion, 163
Crystal plasticity FEM
Simulation of rolling behaviour of cubic oriented al single crystal with crystal plasticity FEM, 79
Cubic oriented Al single crystal
Simulation of rolling behaviour of cubic oriented al single crystal with crystal plasticity FEM, 79
Cure process
Study of cure process of thick solid rubber, 720
Current
Copper and graphite electrodes performance in electrical-discharge machining of XW42 tool steel, 570
Cutting
Laser cutting of thick sheet metals: Effects of cutting parameters on kerf size variations, 285
Cutting force
The influence of different cutting speeds on the cutting force and strain–stress behaviors of single crystal copper during nano-scale orthogonal cutting, 477
Cutting forces
Increase of material removal rate in peripheral milling by varying feed rate, 486

3-D FE modelling
Geometrical effects on residual stresses in 7050-T7451 aluminum alloy rods subject to laser shock peening, 303
Deburring tool
Development of deburring tool for burrs at intersecting holes, 454
Defects occurrence
The experimental study on the defects occurrence of SL mold in injection molding, 706
DEFORM
Application of CAE in cold forging and heat treatment processes for manufacturing of precision helical gear part, 25
Delamination
Effects of peripheral drilling moment on delamination using special drill bits, 471
Design-for-manufacture
Designing using manufacturing feature library, 204
Die angle
An investigation into the effect of redundant shear deformation in bar drawing, 133
Die casting
Tensile behaviour and fracture characteristics of die cast magnesium alloy AM50, 364
Die corner radius
A study of improving warped characteristics during flange forging, 14
Die design
Process analysis and die design in 12 cells condenser tube extrusion of Al3003, 53
Die failure
The die failure prediction and prevention of the orbital forging process, 9
Die life
Die life prediction considering thermal fluid flow and solidification phenomenon in rheology process, 336
Die stress analysis
The die failure prediction and prevention of the orbital forging process, 9
Die-casting process
The molding analysis of automobile parts using the die-casting system, 635
Dieless drawing
FE analysis of size effect on deformation and heat transfer behavior in microtube dieless drawing, 123
Diffusion bonding
Fabrication of titanium parts by massive diffusion bonding, 280

Direct nanoimprint
Effects of thin film properties on metallic pattern formation by direct nanoimprint, 765
Drop transfer mode
Drop transfer mode prediction in pulse GMAW of aluminum using statistical model, 502
Dry sliding
A comparative study of mechanically mixed layers (MMLs) characteristics of commercial aluminium alloys sliding against alumina and steel sliders, 662
Dual phase steel
Hydraulic bulge testing of dual phase steel tubes produced using a novel processing route, 242
Dual-stage
A novel laser micro/nano-machining system for FPD process, 497
Ductile fracture
Optimization of design parameters using a response surface method in a cold cross-wedge rolling, 112
Dynamic FEM
The coupled thermo-mechanical analysis in the upsetting process by the dynamic FEM, 37
Dynamic recrystallization
Hot workability characteristics of cast and homogenized Mg–3Sn–1Ca alloy, 359

ECAP
Superplastic properties of Pb–62%Sn eutectic alloy after equal channel angular pressing (ECAP), 441
Eccentricity
Consideration of buckling characteristics for optimal design of stiffened punch in the blanking process of lead frame, 273
Eccentricity index
Finite element analysis of multi-hole extrusion of aluminum-alloy tubes, 150
EDM
Copper and graphite electrodes performance in electrical-discharge machining of XW42 tool steel, 570
EDS
Effects of heat treatment on the surface of a die steel STD11 machined by W-EDM, 580
Elasto-viscoplastic
Glass material model for the forming stage of the glass molding process, 751
Electric resistance spot weld (ERSW)
Mechanical strength evaluation for Nd-YAG laser and electric resistance spot weld (ERSW) joint under multiaxial loading, 507
Electrical discharge machining (EDM)
Development of a combined machining method using electrorheological fluids for EDM, 565
Electrode wear rate
Copper and graphite electrodes performance in electrical-discharge machining of XW42 tool steel, 570
Electroforming
Processing of PZT actuator and nickel plate in a multi-droplets microejector, 683
Electrorheology (ER)
Development of a combined machining method using electrorheological fluids for EDM, 565
Elliptical hole-flanging process
Analysis of forming limits in metal forming processes, 385
End mill
Planning and analysis of grinding processes for end mills of cemented tungsten carbide, 618
End milling
Behaviors of end milling Inconel 718 superalloy by cemented carbide tools, 460
Experimental study of surface integrity during end milling of Al/SiC particulate metal–matrix composites, 574
Energy
An investigation into the effect of redundant shear deformation in bar drawing, 133
Energy absorption
Effects of notch position of the Charpy impact specimen on the failure behavior in heat affected zone, 419
Engineering simulation
Study of cure process of thick solid rubber, 720
Ensemble modelling
Modelling of hot strip rolling process using a hybrid neural network approach, 101
Etching
Precision blanking of thin sheet metals with the help of chemical etching, 209
Eutectic alloy
Superplastic properties of Pb–62%Sn eutectic alloy after equal channel angular pressing (ECAP), 441
Extracellular secreted metabolites
Metal removal rate of *Thiobacillus thiooxidans* without pre-secreted metabolite, 560
Extruded fin length
An optimum die fillet design for minimizing the difference in extruded fin lengths of straight-fin heat sink extrusion, 145
Extrusion
Application of fuzzy theory to predict deformation behaviors of magnesium alloy sheets under hot extrusion, 138
Extrusion forming process
Finite element analysis of rubber extrusion forming process for automobile weather strip, 168

Failure simulation
Effects of notch position of the Charpy impact specimen on the failure behavior in heat affected zone, 419
Fatigue crack growth rate graph
Some studies on fatigue crack growth rate of aluminum alloy 6061, 380
Fatigue failure
Tool life prediction for the bolt forming process based on high-cycle fatigue and wear, 348
Fatigue life
Effects of microshot peening on surface characteristics of high-speed tool steel, 319
FE
Glass material model for the forming stage of the glass molding process, 751
FE analysis
Process analysis and die design in 12 cells condenser tube extrusion of Al3003, 53
FE analysis of size effect on deformation and heat transfer behavior in microtube dieless drawing, 123
FEM
FE analysis of multi-cycle micro-forming through using closed-die upsetting models and forward extrusion models, 220
FEM (finite element method)
Buckling analysis and test of composite shells under hydrostatic pressure, 742

FEM simulation
Microstructure analysis of aluminum extrusion: Prediction of microstructure on AA6060 alloy, 156
Fiber orientation angle
Measurement of fiber orientation angle in FRP by intensity method, 755
Fiber orientation function
Measurement of fiber orientation angle in FRP by intensity method, 755
Finite element
Numerical-experimental analysis of thin magnesium alloy stripes subjected to stretch-bending, 183
Finite element analysis
Finite element analysis of plastic deformation behavior during high pressure torsion processing, 32
Finite element analysis of multi-hole extrusion of aluminum-alloy tubes, 150
Analysis of plastic flow and die design during extrusion of CPU heat sinks, 174
Tool life prediction for the bolt forming process based on high-cycle fatigue and wear, 348
Finite element method (FEM)
A study on cooling characteristics of tire mold during a manufacturing process of Al–Mg system alloy casting mold, 64
Modelling of friction phenomena in material removal processes, 450
The study of injection/compression liquid composite molding, 695
Finite element modeling and simulation for bending analysis of multi-layer printed circuit boards using woven fiber composite, 746
Finite element simulation
Two-dimensional finite element approximation of the hexagonal bolt forming process, 19
Deformation behavior of the surface defects of low carbon steel in wire rod rolling, 91
Finite-element-analysis
Tool life enhancement in cold forging by locally optimized surfaces, 2
Fixtures
Towards an intelligent fixturing system with rapid reconfiguration and part positioning, 198
Flank wear
Effect of tool holder geometry and cutting condition when milling nickel-based alloy 242, 483
Flaring test
Deformation characteristics of microtubes in flaring test, 214
FLD
Forming limit of AZ31 alloy sheet and strain rate on warm sheet metal forming, 431
Flow behavior
The experimental study on the defects occurrence of SL mold in injection molding, 706
Flow guide
Analysis of plastic flow and die design during extrusion of CPU heat sinks, 174
Flow pattern
The molding analysis of automobile parts using the die-casting system, 635
Flow stress equation
Computer simulation of U-channel for under-rail roll forming using rigid-plastic finite element methods, 118
Flow stress–strain curve
A numerical approach to determine flow stress–strain curve of strip and friction coefficient in actual cold rolling mill, 106
Focused ion beam milling
A study on fabrication of silicon mold for polymer hot-embossing using focused ion beam milling, 548
Form rolling
Micro form rolling: Imprinting ability of microgrooves on metal shafts, 232
Formability
Die design for stamping a notebook case with magnesium alloy sheets, 247
Formability of 6k21-T4 car panel sheet for viscoelastic–plastic flexible-die forming, 408
Formability of steels subjected to cold ECAE process, 390
Forming error
FE analysis of multi-cycle micro-forming through using closed-die upsetting models and forward extrusion models, 220
Forming limit
Forming characteristics of AZ31B magnesium alloy in bidirectional extrusion process, 179
Formability of magnesium AZ31 sheet in the incremental forming at warm temperature, 354
Forming limit of AZ31 alloy sheet and strain rate on warm sheet metal forming, 431
Forming limit ratio
The analysis of forming limit in re-penetration process of the hole-flanging of sheet metal, 256
Analysis of forming limits in metal forming processes, 385
Forming parameters
Analysis of splitting spinning force by the principal stress method, 267
Fractograph
Mechanical properties of the as-cast quartz particulate reinforced LM6 alloy matrix composites, 731
Fractographic analysis
Some studies on fatigue crack growth rate of aluminum alloy 6061, 380
Fracture mode
The processing and fracture analysis on transmission shafts of a peanut harvester, 374
Friction
Modelling of the effect of friction on cold strip rolling, 85
Modelling of friction phenomena in material removal processes, 450
Friction coefficient
A numerical approach to determine flow stress–strain curve of strip and friction coefficient in actual cold rolling mill, 106
Fuzzy prediction system
Application of fuzzy theory to predict deformation behaviors of magnesium alloy sheets under hot extrusion, 138

Gas nitriding
The effects of process variables on the hardness of nitrided 3% chromium steel, 325
Gas turbine
Investigation into thermal stresses in gas turbine transition-piece: Influence of material properties on stress levels, 369
Gibbs free energy
Numerical 3-D FEM simulation of tensor model for liquid crystal displays, 60
Glass molding process
Glass material model for the forming stage of the glass molding process, 751

Glass/metal joining
Application of semisolid joining—Part 4 glass/metal, plastic/metal, or wood/metal joining, 623
Gradient coatings
Structure and mechanical properties of gradient PVD coatings, 310
Grain refinement
Finite element analysis of plastic deformation behavior during high pressure torsion processing, 32
Effect of grain refinement of magnesium alloy AZ31 by severe plastic deformation on material characteristics, 436
Grain size
Microstructure analysis of aluminum extrusion: Prediction of microstructure on AA6060 alloy, 156
Study of thickness and grain size effects on material behavior in micro-forming, 237
Effects of thin film properties on metallic pattern formation by direct nanoimprint, 765
Grinding
Temperature measurement and heat flux characterization in grinding using thermography, 590
Performances of metal-bond diamond tools in grinding alumina, 612
Grinding process
Mechanical properties and grinding performance on aluminum-based metal matrix composites, 596
Planning and analysis of grinding processes for end mills of cemented tungsten carbide, 618

Hardened steel AISI D2
Effects of workpiece preheating on surface roughness, chatter and tool performance during end milling of hardened steel D2, 466
Hardening exponent
Effect of hardening exponent on tube bending, 189
Hardness
Microstructural and hardness investigation of hot-work tool steels by laser surface treatment, 342
Hardness loop
The effects of process variables on the hardness of nitrided 3% chromium steel, 325
Hardness profile
The effects of process variables on the hardness of nitrided 3% chromium steel, 325
Heat flux
Temperature measurement and heat flux characterization in grinding using thermography, 590
Heat treatment
Investigation into thermal stresses in gas turbine transition-piece: Influence of material properties on stress levels, 369
Effects of heat treatment on the surface of a die steel STD11 machined by W-EDM, 580
Heat treatment simulation
Application of CAE in cold forging and heat treatment processes for manufacturing of precision helical gear part, 25
Helical gear
Application of CAE in cold forging and heat treatment processes for manufacturing of precision helical gear part, 25
High pressure die casting (HPDC)
Integrated optimization system for high pressure die casting processes, 629
High pressure torsion
Finite element analysis of plastic deformation behavior during high pressure torsion processing, 32
High speed cutting
Behaviors of end milling Inconel 718 superalloy by cemented carbide tools, 460
High-energy ion beam
Application of ion irradiation for surface finish of micro-forming die, 315
High-speed tool steel
Effects of microshot peening on surface characteristics of high-speed tool steel, 319
Hole-flanging
The analysis of forming limit in re-penetration process of the hole-flanging of sheet metal, 256
Hot bar rolling
Plastic work approach for surface defect prediction in the hot bar rolling process, 73
Hot extrusion
Process analysis and die design in 12 cells condenser tube extrusion of Al3003, 53
Hot rolling process
The processing and fracture analysis on transmission shafts of a peanut harvester, 374
Hot working
Hot workability characteristics of cast and homogenized Mg–3Sn–1Ca alloy, 359
Hot-embossing
A study on fabrication of silicon mold for polymer hot-embossing using focused ion beam milling, 548
Hot-rolled alloy strip
Modelling of hot strip rolling process using a hybrid neural network approach, 101
Hot-work tool steel
Microstructural and hardness investigation of hot-work tool steels by laser surface treatment, 342
Hydroforming
Hydraulic bulge testing of dual phase steel tubes produced using a novel processing route, 242
Hydrostatic extrusion
Backward can extrusion of ultra-fine-grained bulk Al–Mg alloy fabricated by cryomilling and hydrostatic extrusion, 163

IFEM
Prediction of work-hardening coefficient and exponential by adaptive inverse finite element method for tubular material, 413
Image processing
Measurement of fiber orientation angle in FRP by intensity method, 755
Image recognition
Computer-integrated micro-assembling with image-servo system for a microdroplet ejector, 689
Impact damage resistance
Impact damage resistance of sandwich structure subjected to low velocity impact, 425
Impeller
Effect of grain refinement of magnesium alloy AZ31 by severe plastic deformation on material characteristics, 436
IN738
FEM analysis of ultrasonic-vibration-assisted turning and the vibratory tool, 43
Inclined exit surface
Development of deburring tool for burrs at intersecting holes, 454

Inconel 718
Behaviors of end milling Inconel 718 superalloy by cemented carbide tools, 460
Microstructures and mechanical properties of Inconel 718 welds by CO_2 laser welding, 515
Incremental forming
Formability of magnesium AZ31 sheet in the incremental forming at warm temperature, 354
Infrared thermography
Integrated optimization system for high pressure die casting processes, 629
Inhomogeneous deformation
Inhomogeneous deformation and residual stress in skin-pass axisymmetric drawing, 128
Injection molding
The experimental study on the defects occurrence of SL mold in injection molding, 706
Prediction of charging rate in ultrasonic vibration of injection molding, 710
In_2S_3
Simple chemical method for nanoporous network of In_2S_3 platelets for buffer layer in CIS solar cells, 775
Instability
Deformation characteristics of microtubes in flaring test, 214
Insulation
Development of microwave foaming method for phenolic insulation foams, 716
Intensity method
Measurement of fiber orientation angle in FRP by intensity method, 755
Interfacial bonding
Mechanical properties of the as-cast quartz particulate reinforced LM6 alloy matrix composites, 731
Internal stresses
Effects of internal stresses on the mechanical properties of deposition thin films, 770
Intersecting hole
Development of deburring tool for burrs at intersecting holes, 454
Inverse analysis
A study on robust optimization of layered plates bonding process based on inverse analysis, 261
Inverse method
Temperature measurement and heat flux characterization in grinding using thermography, 590
Inverse scheme
A numerical approach to determine flow stress–strain curve of strip and friction coefficient in actual cold rolling mill, 106

316L
Modelling of friction phenomena in material removal processes, 450
Laser
Laser cutting of thick sheet metals: Effects of cutting parameters on kerf size variations, 285
Investigation of laser remote welding using disc laser, 521
Laser alloying process
Ti6Al4V laser alloying process monitoring by using adaptive neural network controller, 297
Laser machining
A novel laser micro/nano-machining system for FPD process, 497
Laser processing
Laser surface treatment of multicrystalline silicon for enhancing optical properties, 291
Laser surface treatment
Microstructural and hardness investigation of hot-work tool steels by laser surface treatment, 342
Laser treatment
Effects of the laser treatment and thermal oxidation behavior of CoNiCrAlY/ZrO_2–8 wt%Y_2O_3 thermal barrier coating, 331
Laser weld
Mechanical strength evaluation for Nd-YAG laser and electric resistance spot weld (ERSW) joint under multiaxial loading, 507
Layer plates bonding
A study on robust optimization of layered plates bonding process based on inverse analysis, 261
Lead frame
Consideration of buckling characteristics for optimal design of stiffened punch in the blanking process of lead frame, 273
Line detection
Computer-integrated micro-assembling with image-servo system for a microdroplet ejector, 689
Linear motor
A novel laser micro/nano-machining system for FPD process, 497
Liquid composite molding
The study of injection/compression liquid composite molding, 695
Local induction hardening
The processing and fracture analysis on transmission shafts of a peanut harvester, 374
Low velocity impact
Impact damage resistance of sandwich structure subjected to low velocity impact, 425
Low voltage inverter
Cost-effective power converter for thin film solar cell technology and improved power quality, 786
LSP process
Geometrical effects on residual stresses in 7050-T7451 aluminum alloy rods subject to laser shock peening, 303
LZ91 magnesium–lithium alloy sheet
Die design for stamping a notebook case with magnesium alloy sheets, 247

Machining
FEM analysis of ultrasonic-vibration-assisted turning and the vibratory tool, 43
Machining effect of the autofrettaged compound cylinder under varying overstrain levels, 491
Macro meso-scopic elastic–plastic behavior
Numerical analysis of influence of micro-parameters on macro-micromechanical properties of fiber reinforced metal matrix composites, 736
Magnesium
Formability of magnesium AZ31 sheet in the incremental forming at warm temperature, 354
Magnesium alloy
Hot workability characteristics of cast and homogenized Mg–3Sn–1Ca alloy, 359
Effect of grain refinement of magnesium alloy AZ31 by severe plastic deformation on material characteristics, 436
Magnesium alloy AM50
Tensile behaviour and fracture characteristics of die cast magnesium alloy AM50, 364

Magnesium alloy sheet
Application of fuzzy theory to predict deformation behaviors of magnesium alloy sheets under hot extrusion, 138
Magnetic field
Fundamental performance of magnetic compound fluid polishing liquid in contact-free polishing of metal surface, 536
Magnetostrictive
Study on advanced multilayered magnetostrictive thin film coating techniques for MEMS application, 678
Mannesmann hole
Optimization of design parameters using a response surface method in a cold cross-wedge rolling, 112
Manufacturing feature library
Designing using manufacturing feature library, 204
Martensitic transformation
Micromechanics model of martensitic transformation-induced plasticity, 226
Massive diffusion bonding
Fabrication of titanium parts by massive diffusion bonding, 280
Material behavior
Study of thickness and grain size effects on material behavior in micro-forming, 237
Deformation characteristics of microtubes in flaring test, 214
Material characteristics
Effect of grain refinement of magnesium alloy AZ31 by severe plastic deformation on material characteristics, 436
Material properties
Prediction of work-hardening coefficient and exponential by adaptive inverse finite element method for tubular material, 413
Material removal rate
Copper and graphite electrodes performance in electrical-discharge machining of XW42 tool steel, 570
Materials
Structure and mechanical properties of gradient PVD coatings, 310
MCF polishing liquid
Fundamental performance of magnetic compound fluid polishing liquid in contact-free polishing of metal surface, 536
Mechanical properties
Modelling of hot strip rolling process using a hybrid neural network approach, 101
Effects of internal stresses on the mechanical properties of deposition thin films, 770
Mechanically mixed layers (MMLs)
A comparative study of mechanically mixed layers (MMLs) characteristics of commercial aluminium alloys sliding against alumina and steel sliders, 662
Meso-scale
Fabrication of meso-scale underwater vehicle components by rapid prototyping process, 640
Metal casting
A study on cooling characteristics of tire mold during a manufacturing process of Al–Mg system alloy casting mold, 64
Metal forming
Effect of hardening exponent on tube bending, 189
Metal matrix composites (MMCs)
Mechanical properties and grinding performance on aluminum-based metal matrix composites, 596
Numerical analysis of influence of micro-parameters on macro-micromechanical properties of fiber reinforced metal matrix composites, 736
Metal removal rate
Metal removal rate of *Thiobacillus thiooxidans* without pre-secreted metabolite, 560
Metal-bond diamond
Performances of metal-bond diamond tools in grinding alumina, 612
Metallic pattern
Effects of thin film properties on metallic pattern formation by direct nanoimprint, 765
Mg alloy sheet
Numerical-experimental analysis of thin magnesium alloy stripes subjected to stretch-bending, 183
Effects of strain rate, temperature and sheet thickness on yield locus of AZ31 magnesium alloy sheet, 395
Micro forming
Micro form rolling: Imprinting ability of microgrooves on metal shafts, 232
Micro screw
Formability of steels subjected to cold ECAE process, 390
Micro-assembly
Computer-integrated micro-assembling with image-servo system for a microdroplet ejector, 689
Microdroplet
Computer-integrated micro-assembling with image-servo system for a microdroplet ejector, 689
Microejector
Processing of PZT actuator and nickel plate in a multi-droplets microejector, 683
Microfissures
Microstructures and mechanical properties of Inconel 718 welds by CO_2 laser welding, 515
Micro-forming
Study of thickness and grain size effects on material behavior in micro-forming, 237
FE analysis of multi-cycle micro-forming through using closed-die upsetting models and forward extrusion models, 220
Microgroove
Micro form rolling: Imprinting ability of microgrooves on metal shafts, 232
Micro-lens array
Tool condition and machined surface monitoring for micro-lens array fabrication in mechanical machining, 585
Micromanufacturing
Surface modification of stainless steel powders for microfabrication, 651
Micromechanics model
Micromechanics model of martensitic transformation-induced plasticity, 226
Micro-parameters
Numerical analysis of influence of micro-parameters on macro-micromechanical properties of fiber reinforced metal matrix composites, 736
Micro-press forming
Application of ion irradiation for surface finish of micro-forming die, 315
Microstructural
Microstructural and hardness investigation of hot-work tool steels by laser surface treatment, 342

Microstructure
Forming characteristics of AZ31B magnesium alloy in bidirectional extrusion process, 179
Microtube
FE analysis of size effect on deformation and heat transfer behavior in microtube dieless drawing, 123
Deformation characteristics of microtubes in flaring test, 214
Microwave
Development of microwave foaming method for phenolic insulation foams, 716
Milling
Increase of material removal rate in peripheral milling by varying feed rate, 486
Modal analysis
Prediction of charging rate in ultrasonic vibration of injection molding, 710
Modelling
Modelling of the effect of friction on cold strip rolling, 85
Moiré interferometry
A study on robust optimization of layered plates bonding process based on inverse analysis, 261
Mold analysis
The molding analysis of automobile parts using the die-casting system, 635
Molecular dynamics
The influence of different cutting speeds on the cutting force and strain–stress behaviors of single crystal copper during nano-scale orthogonal cutting, 477
Molybdenum
Comparison of the influence of molybdenum and chromium TIG surface alloying on the microstructure, hardness and wear resistance of ADI, 673
Moment of inertia
Consideration of buckling characteristics for optimal design of stiffened punch in the blanking process of lead frame, 273
Morphology
A study on characterization of pack-cemented aluminide coating on metals, 669
MR fluid
An investigation of the behaviour of magnetorheological fluids in compression mode, 780
Multi-cell structure
Finite element simulation on superplastic blow forming of diffusion bonded 4 sheets, 68
Multicrystalline silicon
Laser surface treatment of multicrystalline silicon for enhancing optical properties, 291
Multi-cycle loading
FE analysis of multi-cycle micro-forming through using closed-die upsetting models and forward extrusion models, 220
Multi-hole extrusion
Finite element analysis of multi-hole extrusion of aluminum-alloy tubes, 150
Multi-layer
Finite element modeling and simulation for bending analysis of multi-layer printed circuit boards using woven fiber composite, 746
Multilayer
Study on advanced multilayered magnetostrictive thin film coating techniques for MEMS application, 678
Multi-operation stamping
Die design for stamping a notebook case with magnesium alloy sheets, 247

NAK80 mould tool steel
Ultra-precision surface finish of NAK80 mould tool steel using sequential ball burnishing and ball polishing processes, 554
Nano/micro-mold
A study on fabrication of silicon mold for polymer hot-embossing using focused ion beam milling, 548
Nanocrystallinity
Surface modification of stainless steel powders for microfabrication, 651
Nanodiamond
Rheological behavior and tribological performance of a nanodiamond-dispersed lubricant, 542
Nanoindentation
Effects of internal stresses on the mechanical properties of deposition thin films, 770
Nanoindenter
Effects of thin film properties on metallic pattern formation by direct nanoimprint, 765
Nano-scale orthogonal cutting
The influence of different cutting speeds on the cutting force and strain–stress behaviors of single crystal copper during nano-scale orthogonal cutting, 477
Neural network
Modelling of hot strip rolling process using a hybrid neural network approach, 101
Nomex honeycomb sandwich structure
Impact damage resistance of sandwich structure subjected to low velocity impact, 425
Non-Newtonian thermal flow
Finite element analysis of rubber extrusion forming process for automobile weather strip, 168
Non-symmetrical extrusion
Analysis of plastic flow and die design during extrusion of CPU heat sinks, 174
Notch position
Effects of notch position of the Charpy impact specimen on the failure behavior in heat affected zone, 419
Notebook case
Die design for stamping a notebook case with magnesium alloy sheets, 247
Numerical analysis
Numerical analysis of influence of micro-parameters on macro-micromechanical properties of fiber reinforced metal matrix composites, 736
Numerical control
High-accuracy V-bending system by real time identifying material property, 193

Oblateness
Micro form rolling: Imprinting ability of microgrooves on metal shafts, 232
OCB
Numerical 3-D FEM simulation of tensor model for liquid crystal displays, 60
On-line learning
Ti6Al4V laser alloying process monitoring by using adaptive neural network controller, 297
Orbital forging
The die failure prediction and prevention of the orbital forging process, 9

Overstrain level
Machining effect of the autofrettaged compound cylinder under varying overstrain levels, 491

Panels
Formability of 6k21-T4 car panel sheet for viscoelastic–plastic flexible-die forming, 408
Parametric feature
Tool condition and machined surface monitoring for micro-lens array fabrication in mechanical machining, 585
Pb–62%Sn alloy
Superplastic properties of Pb–62%Sn eutectic alloy after equal channel angular pressing (ECAP), 441
Penetration
The analysis of forming limit in re-penetration process of the hole-flanging of sheet metal, 256
Peripheral moment
Effects of peripheral drilling moment on delamination using special drill bits, 471
Permeability
The study of injection/compression liquid composite molding, 695
Phenolic foam
Development of microwave foaming method for phenolic insulation foams, 716
Photochemical analysis
Simple chemical method for nanoporous network of In_2S_3 platelets for buffer layer in CIS solar cells, 775
Photovoltaics
Laser surface treatment of multicrystalline silicon for enhancing optical properties, 291
Piezo actuator
Increase of material removal rate in peripheral milling by varying feed rate, 486
Plastic work approach
Plastic work approach for surface defect prediction in the hot bar rolling process, 73
Plastic/metal joining
Application of semisolid joining—Part 4 glass/metal, plastic/metal, or wood/metal joining, 623
Polishing
Development of a combined machining method using electrorheological fluids for EDM, 565
Poly crystalline cubic boron nitride (PCBN)
Effects of workpiece preheating on surface roughness, chatter and tool performance during end milling of hardened steel D2, 466
Polymer
A study on fabrication of silicon mold for polymer hot-embossing using focused ion beam milling, 548
Poor formability materials
Numerical and experimental confirmation of the calibration stage's effect in multi-operation sheet hydroforming using poor-formability materials, 97
Positioning
Towards an intelligent fixturing system with rapid reconfiguration and part positioning, 198
Post-weld heat treatment
Microstructures and mechanical properties of Inconel 718 welds by CO_2 laser welding, 515
Powder injection molding
Effects of reduction atmosphere and nano carbon powder addition on the deoxidization of injection molded aluminum nitride parts, 701
Powder metallurgy
Processing of PZT actuator and nickel plate in a multi-droplets microejector, 683
Powder properties
The effect of vibratory milling on the powder properties of zinc oxide varistors, 645
Power- and Arrhenious-law models
Finite element analysis of rubber extrusion forming process for automobile weather strip, 168
Preform design
The die failure prediction and prevention of the orbital forging process, 9
Pressureless infiltration
Mechanical properties and grinding performance on aluminum-based metal matrix composites, 596
Principal stress method
Analysis of splitting spinning force by the principal stress method, 267
Printed circuit boards (PCBs)
Finite element modeling and simulation for bending analysis of multi-layer printed circuit boards using woven fiber composite, 746
Process monitoring
State classification of CBN grinding with support vector machine, 601
Processing map
Plastic work approach for surface defect prediction in the hot bar rolling process, 73
Hot workability characteristics of cast and homogenized Mg–3Sn–1Ca alloy, 359
Pulse gas metal arc welding
Drop transfer mode prediction in pulse GMAW of aluminum using statistical model, 502
Pulsing parameters
Drop transfer mode prediction in pulse GMAW of aluminum using statistical model, 502
PVD
Structure and mechanical properties of gradient PVD coatings, 310
PZT actuator
Processing of PZT actuator and nickel plate in a multi-droplets microejector, 683

Q tensor model
Numerical 3-D FEM simulation of tensor model for liquid crystal displays, 60
Quartz particulate
Mechanical properties of the as-cast quartz particulate reinforced LM6 alloy matrix composites, 731
Quasi-isotropic plies
A study on mechanical properties of carbon fiber reinforced plastics by three-point bending testing and transverse static response, 761
Quasi-static axial loading
The energy absorption control characteristics of Al thin-walled tube under quasi-static axial compression, 445

Rapid prototyping (RP)
Fabrication of meso-scale underwater vehicle components by rapid prototyping process, 640
Reconfigurable
Towards an intelligent fixturing system with rapid reconfiguration and part positioning, 198
Recrystallization models
Microstructure analysis of aluminum extrusion: Prediction of microstructure on AA6060 alloy, 156
Reduction atmosphere
Effects of reduction atmosphere and nano carbon powder addition on the deoxidization of injection molded aluminum nitride parts, 701

Redundant deformation factor
An investigation into the effect of redundant shear deformation in bar drawing, 133
Reinforced composite
Effects of laminate sequencing on thermoforming of thermoplastic matrix composites, 725
Remeshing
Two-dimensional finite element approximation of the hexagonal bolt forming process, 19
Remote welding
Investigation of laser remote welding using disc laser, 521
Re-penetration
The analysis of forming limit in re-penetration process of the hole-flanging of sheet metal, 256
Residual strain
Computer simulation of U-channel for under-rail roll forming using rigid-plastic finite element methods, 118
Residual stress
Inhomogeneous deformation and residual stress in skin-pass axisymmetric drawing, 128
Geometrical effects on residual stresses in 7050-T7451 aluminum alloy rods subject to laser shock peening, 303
Response surface method
Optimization of design parameters using a response surface method in a cold cross-wedge rolling, 112
Mechanical properties and grinding performance on aluminum-based metal matrix composites, 596
Rheology
Rheological behavior and tribological performance of a nanodiamond-dispersed lubricant, 542
Rheology forging process
Die life prediction considering thermal fluid flow and solidification phenomenon in rheology process, 336
Rheology material
Die life prediction considering thermal fluid flow and solidification phenomenon in rheology process, 336
Rigid-plastic finite element method
Computer simulation of U-channel for under-rail roll forming using rigid-plastic finite element methods, 118
Ring gap height
A study of improving warped characteristics during flange forging, 14
Robust optimization
A study on robust optimization of layered plates bonding process based on inverse analysis, 261
Roll force
A numerical approach to determine flow stress–strain curve of strip and friction coefficient in actual cold rolling mill, 106
Roll forming
Computer simulation of U-channel for under-rail roll forming using rigid-plastic finite element methods, 118
Rolling
Simulation of rolling behaviour of cubic oriented al single crystal with crystal plasticity FEM, 79

SBR
Study of cure process of thick solid rubber, 720
Self-dressing
Performances of metal-bond diamond tools in grinding alumina, 612
SEM
Simple chemical method for nanoporous network of In_2S_3 platelets for buffer layer in CIS solar cells, 775
Semisolid joining
Application of semisolid joining—Part 4 glass/metal, plastic/metal, or wood/metal joining, 623
Severe plastic deformation
Finite element analysis of plastic deformation behavior during high pressure torsion processing, 32
Shape deposition manufacturing (SDM)
Fabrication of meso-scale underwater vehicle components by rapid prototyping process, 640
Shear
Creasing characteristic of aluminum foil coated paperboard, 401
Shear viscosity
Finite element analysis of rubber extrusion forming process for automobile weather strip, 168
Shear-thinning behaviour
Prediction of charging rate in ultrasonic vibration of injection molding, 710
Sheet hydroforming
Numerical and experimental confirmation of the calibration stage's effect in multi-operation sheet hydroforming using poor-formability materials, 97
Sheet metal forming
Computer simulation of U-channel for under-rail roll forming using rigid-plastic finite element methods, 118
Shot peening
Effects of microshot peening on surface characteristics of high-speed tool steel, 319
Silicon wafer edge
Precision treatment of silicon wafer edge utilizing ultrasonically assisted polishing technique, 531
Simulation
Numerical and experimental confirmation of the calibration stage's effect in multi-operation sheet hydroforming using poor-formability materials, 97
Cost-effective power converter for thin film solar cell technology and improved power quality, 786
Sink mark
Finite element simulation on superplastic blow forming of diffusion bonded 4 sheets, 68
Sintering
Effects of granule size and distribution on the cold isostatic pressed alumina, 657
Size effect
FE analysis of size effect on deformation and heat transfer behavior in microtube dieless drawing, 123
Skin-pass
Inhomogeneous deformation and residual stress in skin-pass axisymmetric drawing, 128
Slug carry-up
Prediction of slug carry-up by the punch in blanking by air-blow of the slug, 252
Smart material
An investigation of the behaviour of magnetorheological fluids in compression mode, 780
Solar cell materials and technologies
Cost-effective power converter for thin film solar cell technology and improved power quality, 786
Special drills
Effects of peripheral drilling moment on delamination using special drill bits, 471
Splitting spinning force
Analysis of splitting spinning force by the principal stress method, 267

Spray-dried granules
Effects of granule size and distribution on the cold isostatic pressed alumina, 657
Spring-back
Numerical-experimental analysis of thin magnesium alloy stripes subjected to stretch-bending, 183
High-accuracy V-bending system by real time identifying material property, 193
Square cup drawing
Forming limit of AZ31 alloy sheet and strain rate on warm sheet metal forming, 431
Square cup drawing process
Analysis of forming limits in metal forming processes, 385
Square thin-walled tube
The energy absorption control characteristics of Al thin-walled tube under quasi-static axial compression, 445
Stainless steel
Surface modification of stainless steel powders for microfabrication, 651
Steel
Formability of steels subjected to cold ECAE process, 390
Straight-fin heat sink
An optimum die fillet design for minimizing the difference in extruded fin lengths of straight-fin heat sink extrusion, 145
Strain rate
Forming limit of AZ31 alloy sheet and strain rate on warm sheet metal forming, 431
Superplastic properties of Pb–62%Sn eutectic alloy after equal channel angular pressing (ECAP), 441
Strain–stress
The influence of different cutting speeds on the cutting force and strain–stress behaviors of single crystal copper during nano-scale orthogonal cutting, 477
Stretching
Numerical-experimental analysis of thin magnesium alloy stripes subjected to stretch-bending, 183
Striation
Laser cutting of thick sheet metals: Effects of cutting parameters on kerf size variations, 285
Superplastic blow forming
Finite element simulation on superplastic blow forming of diffusion bonded 4 sheets, 68
Superplastic forming
Fabrication of titanium parts by massive diffusion bonding, 280
Surface alloying
Comparison of the influence of molybdenum and chromium TIG surface alloying on the microstructure, hardness and wear resistance of ADI, 673
Surface crack
Plastic work approach for surface defect prediction in the hot bar rolling process, 73
Forming characteristics of AZ31B magnesium alloy in bidirectional extrusion process, 179
Surface defect
Deformation behavior of the surface defects of low carbon steel in wire rod rolling, 91
Surface failure
Creasing characteristic of aluminum foil coated paperboard, 401
Surface integrity
Experimental study of surface integrity during end milling of Al/SiC particulate metal–matrix composites, 574
Surface roughness
Application of ion irradiation for surface finish of micro-forming die, 315
Precision treatment of silicon wafer edge utilizing ultrasonically assisted polishing technique, 531
Effects of heat treatment on the surface of a die steel STD11 machined by W-EDM, 580
Surface treatment
Tool life enhancement in cold forging by locally optimized surfaces, 2
A study of improving warped characteristics during flange forging, 14
Laser surface treatment of multicrystalline silicon for enhancing optical properties, 291
System optimization
Integrated optimization system for high pressure die casting processes, 629

7050-T7451 aluminium alloy
Geometrical effects on residual stresses in 7050-T7451 aluminum alloy rods subject to laser shock peening, 303
Taguchi method
An optimum die fillet design for minimizing the difference in extruded fin lengths of straight-fin heat sink extrusion, 145
Taguchi's method
Ultra-precision surface finish of NAK80 mould tool steel using sequential ball burnishing and ball polishing processes, 554
Temperature
Forming limit of AZ31 alloy sheet and strain rate on warm sheet metal forming, 431
Tempering
The effects of process variables on the hardness of nitrided 3% chromium steel, 325
Tensile and fracture behaviours
Tensile behaviour and fracture characteristics of die cast magnesium alloy AM50, 364
Texture
Simulation of rolling behaviour of cubic oriented al single crystal with crystal plasticity FEM, 79
Thermal barrier coating (TBC)
Effects of the laser treatment and thermal oxidation behavior of CoNiCrAlY/ZrO_2–8 wt%Y_2O_3 thermal barrier coating, 331
Thermal stress
Investigation into thermal stresses in gas turbine transition-piece: Influence of material properties on stress levels, 369
Thermally grown oxide (TGO)
Effects of the laser treatment and thermal oxidation behavior of CoNiCrAlY/ZrO_2–8 wt%Y_2O_3 thermal barrier coating, 331
Thermoforming
Effects of laminate sequencing on thermoforming of thermoplastic matrix composites, 725
Thermography
Temperature measurement and heat flux characterization in grinding using thermography, 590
Thermo-mechanical
The coupled thermo-mechanical analysis in the upsetting process by the dynamic FEM, 37
Thermoplastic laminate
Effects of laminate sequencing on thermoforming of thermoplastic matrix composites, 725
Thick sheets
Laser cutting of thick sheet metals: Effects of cutting parameters on kerf size variations, 285

Thickness
Study of thickness and grain size effects on material behavior in micro-forming, 237
Thin films
Study on advanced multilayered magnetostrictive thin film coating techniques for MEMS application, 678
Effects of internal stresses on the mechanical properties of deposition thin films, 770
Thin sheet metals
Precision blanking of thin sheet metals with the help of chemical etching, 209
Three-dimensional projected areas
Analysis of splitting spinning force by the principal stress method, 267
Thrust force
Effects of peripheral drilling moment on delamination using special drill bits, 471
TIG welding
The effect of welding conditions according to mechanical properties of pure titanium, 526
Tire mold
A study on cooling characteristics of tire mold during a manufacturing process of Al–Mg system alloy casting mold, 64
Titanium
The effect of welding conditions according to mechanical properties of pure titanium, 526
Titanium alloys
Fabrication of titanium parts by massive diffusion bonding, 280
Tool design
Design of rotary ultrasonic milling tool using FEM simulation, 48
Tool holder geometry
Effect of tool holder geometry and cutting condition when milling nickel-based alloy 242, 483
Tool life
Tool life enhancement in cold forging by locally optimized surfaces, 2
Tool life prediction for the bolt forming process based on high-cycle fatigue and wear, 348
Effect of tool holder geometry and cutting condition when milling nickel-based alloy 242, 483
Tool materials
Structure and mechanical properties of gradient PVD coatings, 310
Tool wear and surface finish
Effects of workpiece preheating on surface roughness, chatter and tool performance during end milling of hardened steel D2, 466
Torsion fatigue
The processing and fracture analysis on transmission shafts of a peanut harvester, 374
Total thickness variation
A process model of wafer thinning by diamond grinding, 606
Transcription ratio
Micro form rolling: Imprinting ability of microgrooves on metal shafts, 232
Transformation-induced plasticity
Micromechanics model of martensitic transformation-induced plasticity, 226
Transition-piece
Investigation into thermal stresses in gas turbine transition-piece: Influence of material properties on stress levels, 369
Tribometer
Modelling of friction phenomena in material removal processes, 450
Tube bending
Effect of hardening exponent on tube bending, 189
Tube forming
Effect of hardening exponent on tube bending, 189
Hydraulic bulge testing of dual phase steel tubes produced using a novel processing route, 242
Tube-hydroforming
Prediction of work-hardening coefficient and exponential by adaptive inverse finite element method for tubular material, 413
Turning operations
Modelling of friction phenomena in material removal processes, 450

Ultra-fine-grained bulk metal
Backward can extrusion of ultra-fine-grained bulk Al–Mg alloy fabricated by cryomilling and hydrostatic extrusion, 163
Ultrasonic assisted turning
FEM analysis of ultrasonic-vibration-assisted turning and the vibratory tool, 43
Ultrasonic milling
Design of rotary ultrasonic milling tool using FEM simulation, 48
Ultrasonic simulation
Design of rotary ultrasonic milling tool using FEM simulation, 48
Ultrasonic vibration
Prediction of charging rate in ultrasonic vibration of injection molding, 710
Ultrasonically assisted polishing
Precision treatment of silicon wafer edge utilizing ultrasonically assisted polishing technique, 531
Underwater vehicle
Fabrication of meso-scale underwater vehicle components by rapid prototyping process, 640
Upsetting
The coupled thermo-mechanical analysis in the upsetting process by the dynamic FEM, 37

Vacuum plasma spray (VPS)
Effects of the laser treatment and thermal oxidation behavior of CoNiCrAlY/ZrO_2–8 wt%Y_2O_3 thermal barrier coating, 331
Variable speed method
Application of fuzzy theory to predict deformation behaviors of magnesium alloy sheets under hot extrusion, 138
V-bending
High-accuracy V-bending system by real time identifying material property, 193
Vibration
FEM analysis of ultrasonic-vibration-assisted turning and the vibratory tool, 43
Vibration frequency spectrum
Performances of metal-bond diamond tools in grinding alumina, 612
Vibratory milling
The effect of vibratory milling on the powder properties of zinc oxide varistors, 645
Viscoelastic–plastic flexible-die forming
Formability of 6k21-T4 car panel sheet for viscoelastic–plastic flexible-die forming, 408

Viscosity
Die life prediction considering thermal fluid flow and solidification phenomenon in rheology process, 336
Voice coil motor
A novel laser micro/nano-machining system for FPD process, 497
Volume fraction
Mechanical properties of the as-cast quartz particulate reinforced LM6 alloy matrix composites, 731

Wafer grinding process model
A process model of wafer thinning by diamond grinding, 606
Wafer thinning
A process model of wafer thinning by diamond grinding, 606
Warm peening
Effects of microshot peening on surface characteristics of high-speed tool steel, 319
Warm press-forming
Effects of strain rate, temperature and sheet thickness on yield locus of AZ31 magnesium alloy sheet, 395
Warm sheet forming
Forming limit of AZ31 alloy sheet and strain rate on warm sheet metal forming, 431
Warm temperature
Formability of magnesium AZ31 sheet in the incremental forming at warm temperature, 354
Warping phenomenon
A study of improving warped characteristics during flange forging, 14
Waveform factors
Drop transfer mode prediction in pulse GMAW of aluminum using statistical model, 502
Wear
Tool life prediction for the bolt forming process based on high-cycle fatigue and wear, 348
Weather strip
Finite element analysis of rubber extrusion forming process for automobile weather strip, 168
W-EDM
Effects of heat treatment on the surface of a die steel STD11 machined by W-EDM, 580
Weldability
The effect of welding conditions according to mechanical properties of pure titanium, 526
Welding
The effect of welding conditions according to mechanical properties of pure titanium, 526
Welding characteristics
Investigation of laser remote welding using disc laser, 521
Welding condition
The effect of welding conditions according to mechanical properties of pure titanium, 526
Wiping
Numerical-experimental analysis of thin magnesium alloy stripes subjected to stretch-bending, 183
Wire rod
Deformation behavior of the surface defects of low carbon steel in wire rod rolling, 91
Wood/metal joining
Application of semisolid joining—Part 4 glass/metal, plastic/metal, or wood/metal joining, 623
Working area
Investigation of laser remote welding using disc laser, 521
Woven fiber
Finite element modeling and simulation for bending analysis of multi-layer printed circuit boards using woven fiber composite, 746

X-ray diffraction
Study on advanced multilayered magnetostrictive thin film coating techniques for MEMS application, 678

Yield criterion
Effects of strain rate, temperature and sheet thickness on yield locus of AZ31 magnesium alloy sheet, 395
Yield locus
Effects of strain rate, temperature and sheet thickness on yield locus of AZ31 magnesium alloy sheet, 395

Zirconium concentration
The effect of vibratory milling on the powder properties of zinc oxide varistors, 645
ZnO varistor
The effect of vibratory milling on the powder properties of zinc oxide varistors, 645

JOURNAL OF MATERIALS PROCESSING TECHNOLOGY 201 (2008) IX–XV

ELSEVIER

available at www.sciencedirect.com

ScienceDirect

journal homepage: www.elsevier.com/locate/jmatprotec

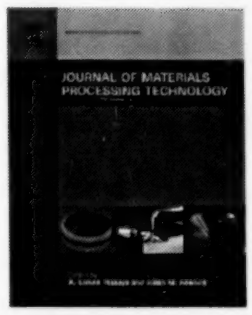

CONTENTS

Preface

Preface 1
Y.T. Im

Forging

Tool life enhancement in cold forging by locally optimized surfaces 2
K. Wagner, R. Völkl, U. Engel

The die failure prediction and prevention of the orbital forging process 9
J.J. Sheu, C.H. Yu

A study of improving warped characteristics during flange forging 14
H.-L. Ho, S.-H. Hsiang, C.-J. Chang

Two-dimensional finite element approximation of the hexagonal bolt forming process 19
H.C. Lee, M.A. Saroosh, Y.T. Im, H.S. Kim, I.H. Son, D.L. Lee

FEA

Application of CAE in cold forging and heat treatment processes for manufacturing of precision helical gear part 25
S.-Y. Kim, S. Kubota, M. Yamanaka

Finite element analysis of plastic deformation behavior during high pressure torsion processing 32
S.C. Yoon, Z. Horita, H.S. Kim

The coupled thermo-mechanical analysis in the upsetting process by the dynamic FEM 37
C.-H. Liu, A.-C. Wang, Y.-S. Chen, C.-M. Wang

FEM analysis of ultrasonic-vibration-assisted turning and the vibratory tool 43
S. Amini, H. Soleimanimehr, M.J. Nategh, A. Abudollah, M.H. Sadeghi

Design of rotary ultrasonic milling tool using FEM simulation 48
K.-L. Kuo

Process analysis and die design in 12 cells condenser tube extrusion of Al3003 53
S.H. Lee, J.M. Lee, H.H. Jo, H. Jo, B.M. Kim

Numerical 3-D FEM simulation of tensor model for liquid crystal displays 60
W.-J. Shin, S.-Y. Cho, J.-B. Lee, T. Won

A study on cooling characteristics of tire mold during a manufacturing process of Al–Mg system alloy casting mold 64
H.D. Yang, Y.K. Oh

Finite element simulation on superplastic blow forming of diffusion bonded 4 sheets 68
J.H. Yoon, H.S. Lee, Y.M. Yi

Plastic work approach for surface defect prediction in the hot bar rolling process 73
M. Awais, H.W. Lee, Y.T. Im, H.C. Kwon, S.M. Byon, H.D. Park

Rolling & Hydroforming

Simulation of rolling behaviour of cubic oriented al single crystal with crystal plasticity FEM 79
L.Y. Si, C. Lu, N.N. Huynh, A.K. Tieu, X.H. Liu

Modelling of the effect of friction on cold strip rolling 85
Z.Y. Jiang, S.W. Xiong, A.K. Tieu, Q. Jane Wang

Elsevier B.V.

Deformation behavior of the surface defects of low carbon steel in wire rod rolling 91
I.H. Son, J.D. Lee, S. Choi, D.L. Lee, Y.T. Im

Numerical and experimental confirmation of the calibration stage's effect in multi-operation sheet hydroforming using poor-formability materials 97
L. Lang, G. Gu, T. Li, X. Zhou

Modelling of hot strip rolling process using a hybrid neural network approach 101
H.J. Kim, M. Mahfouf, Y.Y. Yang

A numerical approach to determine flow stress–strain curve of strip and friction coefficient in actual cold rolling mill 106
S.M. Byon, S.I. Kim, Y. Lee

Optimization of design parameters using a response surface method in a cold cross-wedge rolling 112
H.W. Lee, G.A. Lee, D.J. Yoon, S. Choi, K.H. Na, M.Y. Hwang

Computer simulation of U-channel for under-rail roll forming using rigid-plastic finite element methods ... 118
S.H. Jeong, S.H. Lee, G.H. Kim, H.J. Seo, T.H. Kim

Drawing

FE analysis of size effect on deformation and heat transfer behavior in microtube dieless drawing 123
T. Furushima, K. Manabe

Inhomogeneous deformation and residual stress in skin-pass axisymmetric drawing 128
H.-S. Lin, Y.-C. Hsu, C.-C. Keh

An investigation into the effect of redundant shear deformation in bar drawing 133
G.H. Majzoobi, F.F. Saniee, A. Aghili

Extrusion

Application of fuzzy theory to predict deformation behaviors of magnesium alloy sheets under hot extrusion 138
S.H. Hsiang, Y.W. Lin

An optimum die fillet design for minimizing the difference in extruded fin lengths of straight-fin heat sink extrusion 145
C.-T. Kwan, F.-S. Jan, W.-C. Lee

Finite element analysis of multi-hole extrusion of aluminum-alloy tubes 150
F.-K. Chen, W.-C. Chuang, S. Torng

Microstructure analysis of aluminum extrusion: Prediction of microstructure on AA6060 alloy 156
M. Schikorra, L. Donati, L. Tomesani, A.E. Tekkaya

Backward can extrusion of ultra-fine-grained bulk Al–Mg alloy fabricated by cryomilling and hydrostatic extrusion 163
E.-Z. Kim, S.-I. Oh, Y.-S. Lee, K.-H. Na

Finite element analysis of rubber extrusion forming process for automobile weather strip 168
Y.S. Ha, J.R. Cho, T.H. Kim, J.H. Kim

Analysis of plastic flow and die design during extrusion of CPU heat sinks 174
Y.M. Hwang, C.Y. Shen

Forming characteristics of AZ31B magnesium alloy in bidirectional extrusion process 179
D.J. Yoon, S.J. Lim, H.G. Jeong, E.Z. Kim, C.D. Cho

Bending & CAD

Numerical-experimental analysis of thin magnesium alloy stripes subjected to stretch-bending 183
G. Palumbo, D. Sorgente, L. Tricarico

Effect of hardening exponent on tube bending 189
M. Murata, T. Kuboki, K. Takahashi, M. Goodarzi, Y. Jin

High-accuracy V-bending system by real time identifying material property 193
K. Imai, J. Koyama, Y. Jin

Towards an intelligent fixturing system with rapid reconfiguration and part positioning 198
M. Ryll, T.N. Papastathis, S. Ratchev

Designing using manufacturing feature library 204
A.S.M. Hoque, T. Szecsi

Microforming

Precision blanking of thin sheet metals with the help of chemical etching 209
K. Hirota, Y. Tsukiyama, T. Yasuumi

Deformation characteristics of microtubes in flaring test 214
M.A. Mirzai, K.-i. Manabe, T. Mabuchi

FE analysis of multi-cycle micro-forming through using closed-die upsetting models and forward extrusion models 220
W. Pan, Y. Qin

Micromechanics model of martensitic transformation-induced plasticity 226
C.Y. Sun, G. Fang, L.P. Lei, P. Zeng

Micro form rolling: Imprinting ability of microgrooves on metal shafts..... 232
M. Yamamoto, T. Kuwabara

Study of thickness and grain size effects on material behavior in micro-forming..... 237
F.-H. Yeh, C.-L. Li, Y.-H. Lu

Sheet Metal Forming

Hydraulic bulge testing of dual phase steel tubes produced using a novel processing route..... 242
E.J. Pavlina, C.J. Van Tyne, K. Hertel

Die design for stamping a notebook case with magnesium alloy sheets..... 247
H.-K. Tsai, C.-C. Liao, F.-K. Chen

Prediction of slug carry-up by the punch in blanking by air-blow of the slug..... 252
R.Q. Hsu, J.R. Chang, D.L. Liang

The analysis of forming limit in re-penetration process of the hole-flanging of sheet metal 256
C.-L. Li, Y.-M. Huang, Y.-W. Tsai

A study on robust optimization of layered plates bonding process based on inverse analysis 261
J.-Y. Kim, J.-H. Choi, J.-W. Joo

Analysis of splitting spinning force by the principal stress method..... 267
L. Huang, H. Yang, M. Zhan, Y. Liu

Consideration of buckling characteristics for optimal design of stiffened punch in the blanking process of lead frame 273
D.C. Ko, I.S. Lee, B.M. Kim

Fabrication of titanium parts by massive diffusion bonding 280
H.-S. Lee, J.-H. Yoon, Y.-M. Yi

Laser Processing

Laser cutting of thick sheet metals: Effects of cutting parameters on kerf size variations..... 285
B.S. Yilbas

Laser surface treatment of multicrystalline silicon for enhancing optical properties 291
L.A. Dobrzański, A. Drygała, K. Gołombek, P. Panek, E. Bielańska, P. Zięba

Ti6Al4V laser alloying process monitoring by using adaptive neural network controller 297
H.-Y. Chen, S.-J. Huang

Geometrical effects on residual stresses in 7050-T7451 aluminum alloy rods subject to laser shock peening 303
C. Yang, P.D. Hodgson, Q. Liu, L. Ye

Tool life & Coating

Structure and mechanical properties of gradient PVD coatings..... 310
L.A. Dobrzański, L.W. Żukowska, J. Mikuła, K. Gołombek, D. Pakuła, M. Pancielejko

Application of ion irradiation for surface finish of micro-forming die..... 315
M. Yang, A. Osako

Effects of microshot peening on surface characteristics of high-speed tool steel 319
Y. Harada, K. Fukauara, S. Kohamada

The effects of process variables on the hardness of nitrided 3% chromium steel 325
S. Mridha, A.A. Khan

Effects of the laser treatment and thermal oxidation behavior of CoNiCrAlY/ZrO_2–8 wt%Y_2O_3 thermal barrier coating 331
J.H. Park, J.S. Kim, K.H. Lee, Y.S. Song, M.C. Kang

Die life prediction considering thermal fluid flow and solidification phenomenon in rheology process 336
J.W. Bae, D.Y. Seol, C.G. Kang, S.M. Lee

Microstructural and hardness investigation of hot-work tool steels by laser surface treatment 342
H.J. Shin, Y.T. Yoo

Tool life prediction for the bolt forming process based on high-cycle fatigue and wear 348
H.C. Lee, Y. Lee, S.Y. Lee, S. Choi, D.L. Lee, Y.T. Im

Material Property & Formability

Formability of magnesium AZ31 sheet in the incremental forming at warm temperature 354
Y.H. Ji, J.J. Park

Hot workability characteristics of cast and homogenized Mg–3Sn–1Ca alloy 359
K.P. Rao, Y.V.R.K. Prasad, N. Hort, K.U. Kainer

Tensile behaviour and fracture characteristics of die cast magnesium alloy AM50 364
H. Hu, M. Zhou, Z. Sun, N. Li

Investigation into thermal stresses in gas turbine transition-piece: Influence of material properties on stress levels 369
A.H. Mustafa, M.S. Hashmi, B.S. Yilbas, M. Sunar

The processing and fracture analysis on transmission shafts of a peanut harvester 374
C.-F. Tseng, W.-S. Lin

Some studies on fatigue crack growth rate of aluminum alloy 6061 380
B.F. Jogi, P.K. Brahmankar, V.S. Nanda, R.C. Prasad

Analysis of forming limits in metal forming processes 385
Y.-M. Huang, Y.-W. Tsai, C.-L. Li

Formability of steels subjected to cold ECAE process 390
A. Yanagida, K. Joko, A. Azushima

Effects of strain rate, temperature and sheet thickness on yield locus of AZ31 magnesium alloy sheet 395
T. Naka, T. Uemori, R. Hino, M. Kohzu, K. Higashi, F. Yoshida

Creasing characteristic of aluminum foil coated paperboard 401
S. Nagasawa, R. Endo, Y. Fukuzawa, S. Uchino, I. Katayama

Formability of 6k21-T4 car panel sheet for viscoelastic–plastic flexible-die forming 408
Z. Wang, Y. Li

Prediction of work-hardening coefficient and exponential by adaptive inverse finite element method for tubular material 413
Y. Xu, L.C. Chan, Y.C. Tsien, L. Gao, P.F. Zheng

Effects of notch position of the Charpy impact specimen on the failure behavior in heat affected zone ... 419
Y.C. Jang, J.K. Hong, J.H. Park, D.W. Kim, Y. Lee

Impact damage resistance of sandwich structure subjected to low velocity impact 425
J.H. Park, S.K. Ha, K.W. Kang, C.W. Kim, H.S. Kim

Forming limit of AZ31 alloy sheet and strain rate on warm sheet metal forming 431
Y.S. Lee, Y.N. Kwon, S.H. Kang, S.W. Kim, J.H. Lee

Effect of grain refinement of magnesium alloy AZ31 by severe plastic deformation on material characteristics 436
S.H. Kang, Y.S. Lee, J.H. Lee

Superplastic properties of Pb–62%Sn eutectic alloy after equal channel angular pressing (ECAP) 441
S. Lee

The energy absorption control characteristics of Al thin-walled tube under quasi-static axial compression 445
K.S. Lee, S.K. Kim, I.Y. Yang

Material Removal Process

Modelling of friction phenomena in material removal processes 450
F. Valiorgue, J. Rech, H. Hamdi, C. Bonnet, P. Gilles, J.M. Bergheau

Development of deburring tool for burrs at intersecting holes 454
K.U. Lee, S.L. Ko

Behaviors of end milling Inconel 718 superalloy by cemented carbide tools 460
Y.S. Liao, H.M. Lin, J.H. Wang

Effects of workpiece preheating on surface roughness, chatter and tool performance during end milling of hardened steel D2 466
A.K.M.N. Amin, S.B. Dolah, M.B. Mahmud, M.A. Lajis

Effects of peripheral drilling moment on delamination using special drill bits 471
C.C. Tsao, H. Hocheng

The influence of different cutting speeds on the cutting force and strain–stress behaviors of single crystal copper during nano-scale orthogonal cutting 477
Z.-C. Lin, J.-C. Huang

Effect of tool holder geometry and cutting condition when milling nickel-based alloy 242 483
H.H. Habeeb, K.A. Abou-El-Hossein, B. Mohammad, K. Kadirgama

Increase of material removal rate in peripheral milling by varying feed rate 486
H. Pérez, J. Rios, E. Díez, A. Vizán

Machining effect of the autofrettaged compound cylinder under varying overstrain levels 491
J.-H. Park, Y.-S. Lee, J.-H. Kim, K.-U. Cha, S.-K. Hong

A novel laser micro/nano-machining system for FPD process 497
K. Kim, Y.-M. Choi, D.-G. Gweon, M.G. Lee

Welding

Drop transfer mode prediction in pulse GMAW of aluminum using statistical model 502
P. Praveen, M.J. Kang, P.K.D.V. Yarlagadda

Mechanical strength evaluation for Nd-YAG laser and electric resistance spot weld (ERSW) joint under multiaxial loading 507
H.A. Kavamura, G.F. Batalha

Microstructures and mechanical properties of Inconel 718 welds by CO_2 laser welding 515
J.K. Hong, J.H. Park, N.K. Park, I.S. Eom, M.B. Kim, C.Y. Kang

Investigation of laser remote welding using disc laser 521
C. Kim, J. Kim, H. Lim, J. Kim

The effect of welding conditions according to mechanical properties of pure titanium 526
B.H. Choi, B.K. Choi

Polishing

Precision treatment of silicon wafer edge utilizing ultrasonically assisted polishing technique 531
N. Kobayashi, Y. Wu, M. Nomura, T. Sato

Fundamental performance of magnetic compound fluid polishing liquid in contact-free polishing of metal surface 536
T. Furuya, Y. Wu, M. Nomura, K. Shimada, K. Yamamoto

Rheological behavior and tribological performance of a nanodiamond-dispersed lubricant 542
C.C. Chou, S.H. Lee

Non-traditional Machining

A study on fabrication of silicon mold for polymer hot-embossing using focused ion beam milling 548
S.-W. Youn, C. Okuyama, M. Takahashi, R. Maeda

Ultra-precision surface finish of NAK80 mould tool steel using sequential ball burnishing and ball polishing processes 554
F.J. Shiou, C.H. Cheng

Metal removal rate of *Thiobacillus thiooxidans* without pre-secreted metabolite 560
J.H. Chang, H. Hocheng, H.Y. Chang, A. Shih

Development of a combined machining method using electrorheological fluids for EDM 565
Y.Y. Tsai, C.H. Tseng, C.K. Chang

Copper and graphite electrodes performance in electrical-discharge machining of XW42 tool steel 570
C.H. Che Haron, J.A. Ghani, Y. Burhanuddin, Y.K. Seong, C.Y. Swee

Experimental study of surface integrity during end milling of Al/SiC particulate metal–matrix composites ... 574
N. Suresh Kumar Reddy, S. Kwang-Sup, M. Yang

Effects of heat treatment on the surface of a die steel STD11 machined by W-EDM 580
K.-K. Choi, W.-J. Nam, Y.-S. Lee

Tool condition and machined surface monitoring for micro-lens array fabrication in mechanical machining... 585
I.S. Kang, J.S. Kim, M.C. Kang, K.Y. Lee

Grinding

Temperature measurement and heat flux characterization in grinding using thermography 590
A. Brosse, P. Naisson, H. Hamdi, J.M. Bergheau

Mechanical properties and grinding performance on aluminum-based metal matrix composites..... 596
J.S. Kwak, Y.S. Kim

State classification of CBN grinding with support vector machine..... 601
N.-H. Chiu, Y.-Y. Guao

A process model of wafer thinning by diamond grinding..... 606
C.-C.A. Chen, L.-S. Hsu

Performances of metal-bond diamond tools in grinding alumina..... 612
C.-S. Lin, Y.-L. Yang, S.-T. Lin

Planning and analysis of grinding processes for end mills of cemented tungsten carbide..... 618
J.-Y. Chen, B.-Y. Lee, C.-H. Chen

Casting

Application of semisolid joining—Part 4 glass/metal, plastic/metal, or wood/metal joining 623
S. Sugiyama, M. Kiuchi, J. Yanagimoto

Integrated optimization system for high pressure die casting processes..... 629
L.X. Kong, F.H. She, W.M. Gao, S. Nahavandi, P.D. Hodgson

The molding analysis of automobile parts using the die-casting system 635
B.S. Sung, I.S. Kim

Fabrication of meso-scale underwater vehicle components by rapid prototyping process..... 640
Y.-L. Cheng, J.-H. Lai

The effect of vibratory milling on the powder properties of zinc oxide varistors..... 645
M.C. Kelleher, M.S.J. Hashmi

Surface modification of stainless steel powders for microfabrication 651
M.T. Vieira, A.G. Martins, F.M. Barreiros, M. Matos, J.M. Castanho

Effects of granule size and distribution on the cold isostatic pressed alumina 657
C.-S. Lin, S.-T. Lin

A comparative study of mechanically mixed layers (MMLs) characteristics of commercial aluminium alloys sliding against alumina and steel sliders..... 662
M.J. Ghazali, W.M. Rainforth, M.Z. Omar

A study on characterization of pack-cemented aluminide coating on metals 669
K. Mohammadi, A.K. Haghi

Comparison of the influence of molybdenum and chromium TIG surface alloying on the microstructure, hardness and wear resistance of ADI 673
A. Amirsadeghi, M.H. Sohi

MEMS

Study on advanced multilayered magnetostrictive thin film coating techniques for MEMS application 678
H.-S. Lee, C. Cho

Processing of PZT actuator and nickel plate in a multi-droplets microejector 683
C.H. Cheng, A.S. Yang, T.H. Hsu

Computer-integrated micro-assembling with image-servo system for a microdroplet ejector 689
C.J. Lin, G.Z. Chen, Y.X. Huang, J.K. Chang

Injection Molding

The study of injection/compression liquid composite molding..... 695
C.-H. Wu, Y.-R. Pan

Effects of reduction atmosphere and nano carbon powder addition on the deoxidization of injection molded aluminum nitride parts 701
K.-H. Lin, Y.-C. Lin, S.-T. Lin

The experimental study on the defects occurrence of SL mold in injection molding 706
C.-C. An, R.-H. Chen
Prediction of charging rate in ultrasonic vibration of injection molding 710
J. Lee, N. Kim

Composites
Development of microwave foaming method for phenolic insulation foams 716
B.G. Kim, D.G. Lee
Study of cure process of thick solid rubber 720
S. Nozu, H. Tsuji, M. Itadani, W. Fujiwara, K. Ohnishi
Effects of laminate sequencing on thermoforming of thermoplastic matrix composites 725
M. Sadighi, E. Rabizadeh, F. Kermansaravi
Mechanical properties of the as-cast quartz particulate reinforced LM6 alloy matrix composites 731
S. Sulaiman, M. Sayuti, R. Samin
Numerical analysis of influence of micro-parameters on macro-micromechanical properties of fiber reinforced metal matrix composites 736
L. Hu, S. Zhang, D. Li, Q. Chang, Y. Peng
Buckling analysis and test of composite shells under hydrostatic pressure 742
J.Y. Han, H.Y. Jung, J.R. Cho, J.H. Choi, W.B. Bae
Finite element modeling and simulation for bending analysis of multi-layer printed circuit boards using woven fiber composite 746
L. Li, S.M. Kim, S.H. Song, T.W. Ku, W.J. Song, J. Kim, M.K. Chong, J.W. Park, B.S. Kang
Glass material model for the forming stage of the glass molding process 751
Y.-C. Tsai, C. Hung, J.-C. Hung
Measurement of fiber orientation angle in FRP by intensity method 755
J.W. Kim, D.G. Lee
A study on mechanical properties of carbon fiber reinforced plastics by three-point bending testing and transverse static response 761
S.-C. Lee, S.-T. Jeong, J.-N. Park, S.j. Kim, G.-J. Cho

Thin Film
Effects of thin film properties on metallic pattern formation by direct nanoimprint 765
C.H. Yao, C.L. Wu, C.K. Sung
Effects of internal stresses on the mechanical properties of deposition thin films 770
C.T. Chuang, C.K. Chao, R.C. Chang, K.Y. Chu
Simple chemical method for nanoporous network of In_2S_3 platelets for buffer layer in CIS solar cells 775
I. Puspitasari, T.P. Gujar, K.-D. Jung, O.-S. Joo
An investigation of the behaviour of magnetorheological fluids in compression mode 780
S.A. Mazlan, N.B. Ekreem, A.G. Olabi
Cost-effective power converter for thin film solar cell technology and improved power quality 786
S. Sladić, B. Barišić, M. Soković

Author index 791

Subject index 794